use in Nissl staining. Neighboring sections were treated with 0.2% osmium tetroxide to visualize myelinated structures that facilitated identification of the tissue architecture.

2.4. Analysis

Images of stained materials were digitized by a scanner (GT-X970, SEIKO EPSON, Nagano, Japan) attached to a personal computer (NetVista, IBM Japan, Tokyo, Japan) and stored in TIFF format. The distance between the reference tracks in each section was measured by an application ImageJ (NIH). The tissue architecture was reconstructed three-dimensionally by tracing the contours of different anatomical structures inside individual sections with a computer-assisted neuron tracing system (Neurolucida, MicroBrightField, Williston, USA). Reference tracks were used to align consecutive sections. Three-dimensional view of the reconstructed materials was made possible by the Neuroexplorer Solid modeling module (MicroBrightField).

3. Results

3.1. Preparation of complete serial sections in a short period with the least deformity

Embedding tissues in gelatin and cutting them with a vibrating microtome obviated several difficulties in preparation of histological materials from the human brain. It took just one overnight to embed a large block before cutting, and complete serial sections could be obtained on the following day. This is contrasted with the conventional paraffin or celloidin preparations that require long dehydration procedures lasting weeks to months for large blocks.

The combination of gelatin embedding and use of a vibrating microtome also had advantage in accurate sectioning. Dehydra-

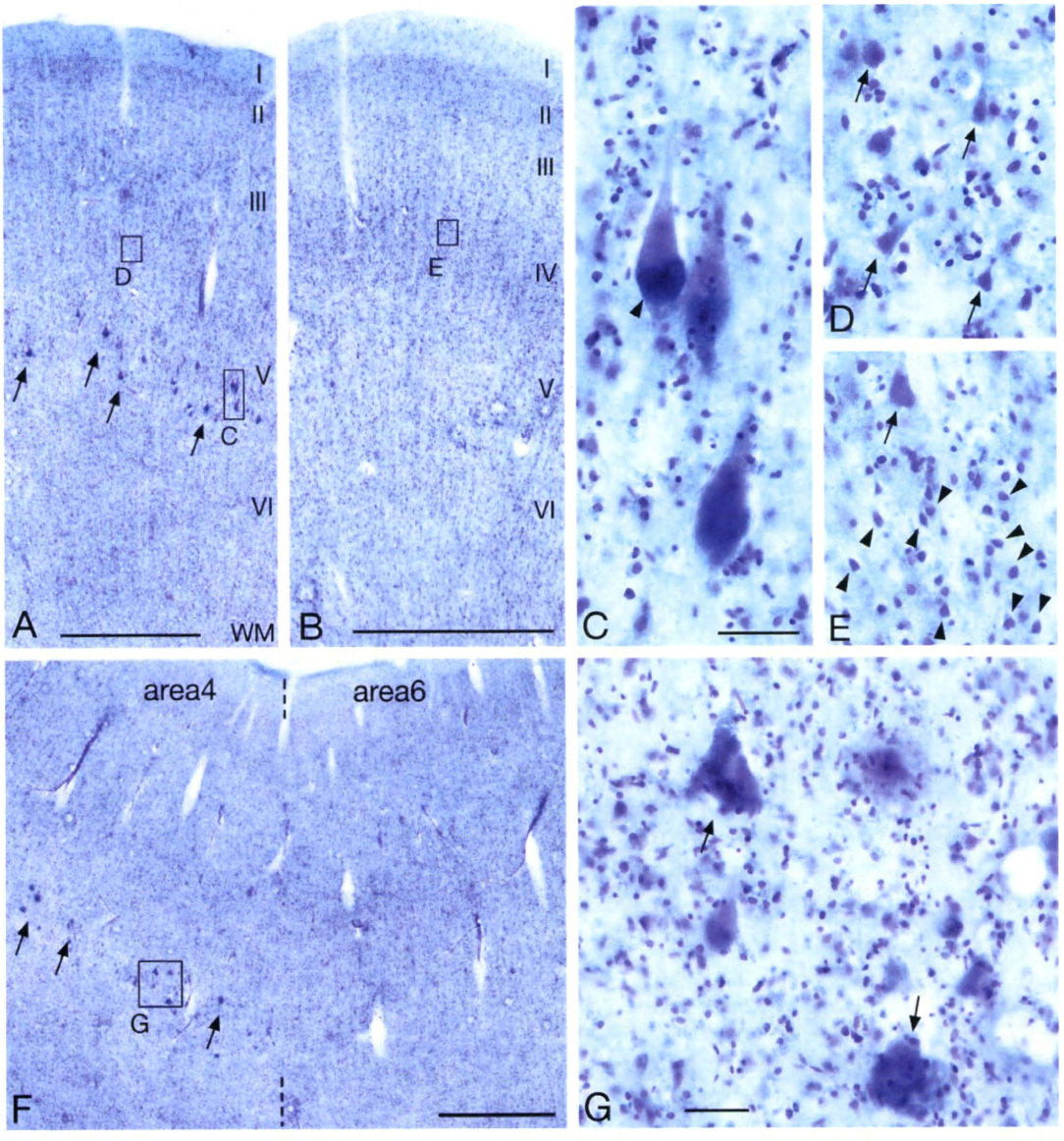

Fig. 3. Light micrographs showing the quality of the staining. (A) Low-power view of the cortical area 4 of Brodmann located in the dorsal part of the precentral gyrus. The position of the tissue inside the original brain is shown by a yellow triangle in Fig. 6. Giant pyramidal cells of Betz (arrows) are seen in layer V, some of which are enlarged in C. The more superficial region around the border to layer III (left box) is shown in D. (B) The postcentral gyrus characterized by the presence of well-developed layer IV, part of which is enlarged in E. (C) Enlargement of the giant pyramidal cells of Betz shown in (A). Lipofuscin granules (arrowhead) are highly accumulated inside the cells. (D) Pyramidal cells of medium to relatively large size are shown by arrows. (E) Enlargement of the upper part of layer IV in B. Arrowheads indicate small, presumptive spiny stellate cells. A pyramidal cell of a large size is located at the bottom of layer III (arrow). (F) The border between area 4 and area 6. Giant pyramidal cells of Betz (arrows) in area 4 disappear abruptly at the border toward the neighboring area6 where agranular laminar pattern is similar to that in area 4. (G) Enlargement of giant pyramidal cells (arrows) in a boxed region in F. Scale bars: 1 mm (A, B, F); 50 μm (C–E, G) (For interpretation of the references to color in this figure legend, the reader is referred to the web version of the article.).

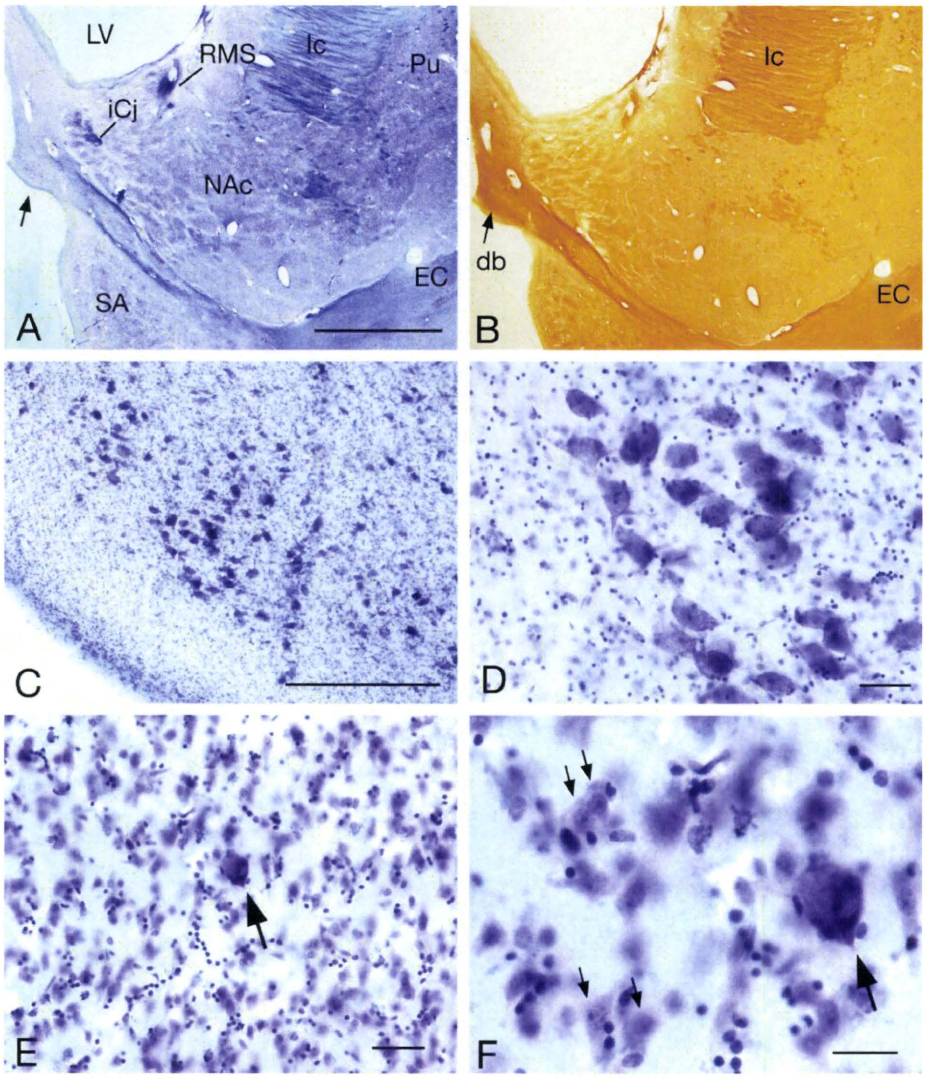

Fig. 4. Light micrographs showing the staining quality in subcortical structures. (A) Low-power view of the region around the accumbens nucleus (NAc). Other structures are: iCj, islands of Calleja; RMS, rostratory migratory stream that could be traced in serial sections to the olfactory tract; LV, lateral ventricle; Ic, internal capsule; Pu, putamen; SA, subcallosal area; EC, external capsule. The arrow at the left side indicates the nucleus of diagonal band that is enlarged in C and D. (B) Myeloarchitecture in the neighboring section stained with osmium tetroxide. Arrow indicates the diagonal band (db). (C and D) The nucleus of diagonal band contains numerous large cells. (E and F) Enlargement of the putamen characterized by medium-sized neurons (small arrows in F) and a much larger, presumptive cholinergic giant aspiny cell (large arrows). Scale bars = 5 mm (A and B); 500 μm (C); 50 μm (D and E); 100 μm (F).

tion before the conventional embedding procedures unavoidably causes shrinkage of the block and the resultant deformity due to the anisotropy in shrinkage. Gelatin embedding in the present method could skip this process. Moreover, as shown in Fig. 2 it also minimized the deformity after cutting. The distances between reference tracks were measured in each section, and the coefficient of variation (standard deviation/mean) was calculated in individual blocks. The distances were found to be kept constant throughout the series; the coefficient was at quite low levels (0.005–0.01, mean 0.008; $n = 10$ blocks).

3.2. 3D reconstruction from serial sections

Thickness of sections was optimized to 100 μm in order to obtain serial preparations. This relatively large thickness did not affect observations of the cytoarchitecture that is unique to and indispensable for the identification of each anatomical region. For example, specific laminar patterns of various neocortical areas could be distinguished (Fig. 3), and the presence of characteristic neuron populations was recognizable in different nuclei (Fig. 4).

Based on the accuracy and quality of the tissue preparation, structures contained in serial sections were traced for 3D-reconstructions by using the computer-assisted system (Fig. 5). As seen in Fig. 5A, the reconstructions had smooth surfaces without any corrections of the traced data. When 1 cm-thick slice had been cut into 2–3 blocks before microtome sectioning, reconstructions from these blocks could be put together to recover the original 1-cm thick slice without the necessity of scaling (Fig. 5B, Supplementary Fig. 1). As the data were stored in a digital format, the complicated 3D morphology of the internal structures such as basal ganglia (Fig. 5C) was observable in different viewing angles (Fig. 6). The 3D view of the recovered slice was then compared with both the non-contact 3D digitizer model and the photograph of the hemisphere to know its original position within the brain. Correspondence of gyri and sulci between the reconstructions and the original brain was recognizable as in Fig. 6. As the digital files for reconstructions are composed of numer-

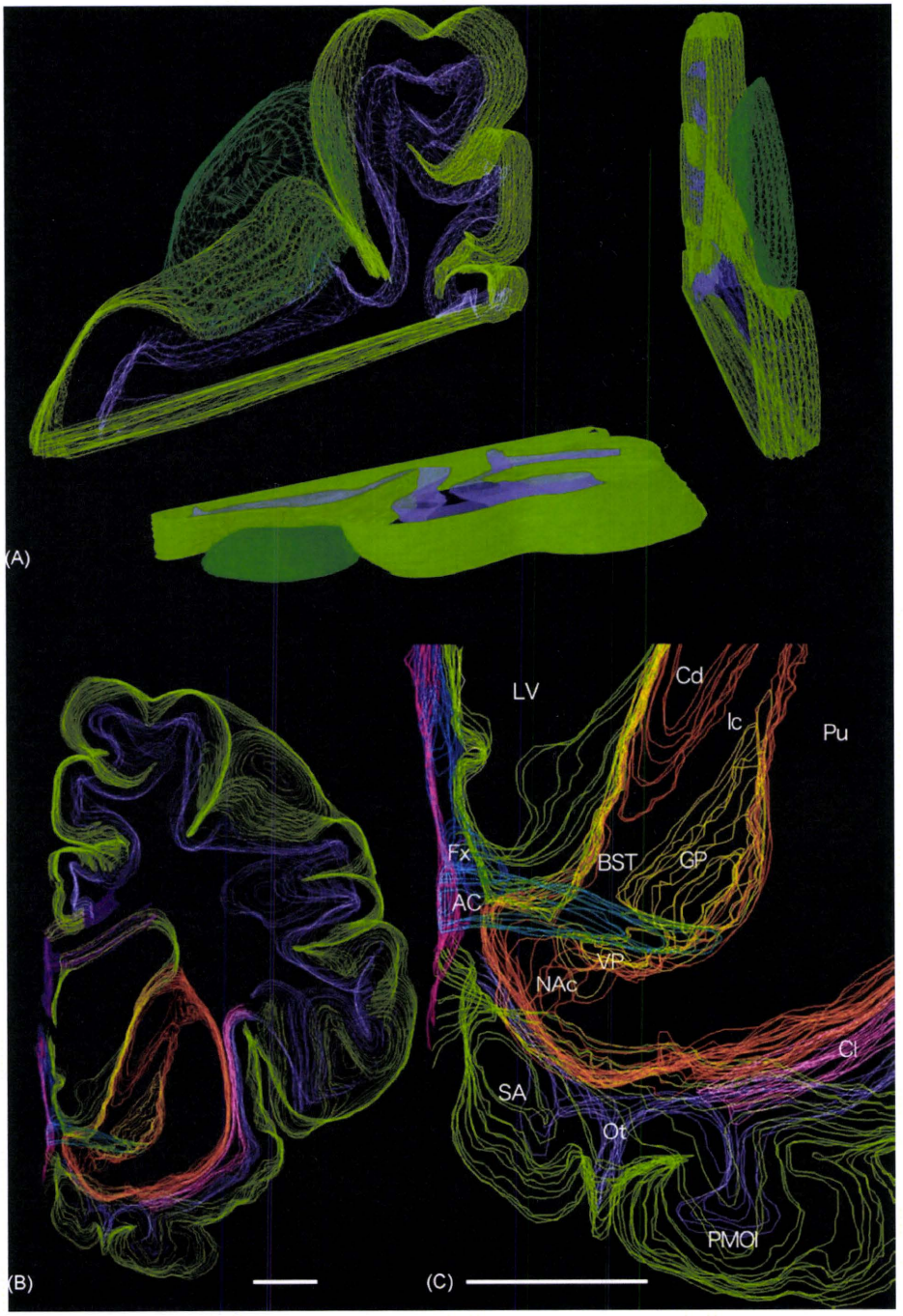

Fig. 5. Reconstruction from the serial sections. (A) Computer-assisted tracings of a brain block near the central sulcus are reconstructed and viewed from different angles. Note smooth surfaces of the reconstructed images that are free from correction of the original tracing data. (B) A composite image of the three reconstructions (Supplementary Fig. 1) that are put together without scaling. (C) Enlargement of a part of (B), indicating various internal architecture: AC, anterior commissure; BST, bed nucleus of stria terminalis; Cd, caudate nucleus; Cl, claustrum; Fx, fornix; GP, globus pallidus; Ot, olfactory tract; PMOl, posteromedial orbital lobule; VP, ventral pallidum. Other abbreviations as Fig. 4. Scale bars: 1 cm.

ous spatial points having 3D coordinates, calculation of the best fit between these data and the coordinates within the 3D digitizer model is possible, which is now in progress (Morooka et al., 2009).

4. Discussion

The present study has established a simple method for preparing serial sections of large-sized brain tissues of the human. Combination of gelatin embedding and use of a vibrating microtome has led to both shortening of time for tissue preparation and minimizing the deformity of the specimens. The obtained sections were processed for Nissl staining that is the standard method for identifying tissue structure of the brain, for which the present materials had enough quality. Moreover, even such a simple staining method has revealed unique tissue architectures in the basal forebrain that was quite different from those in rodents (our unpublished observations).

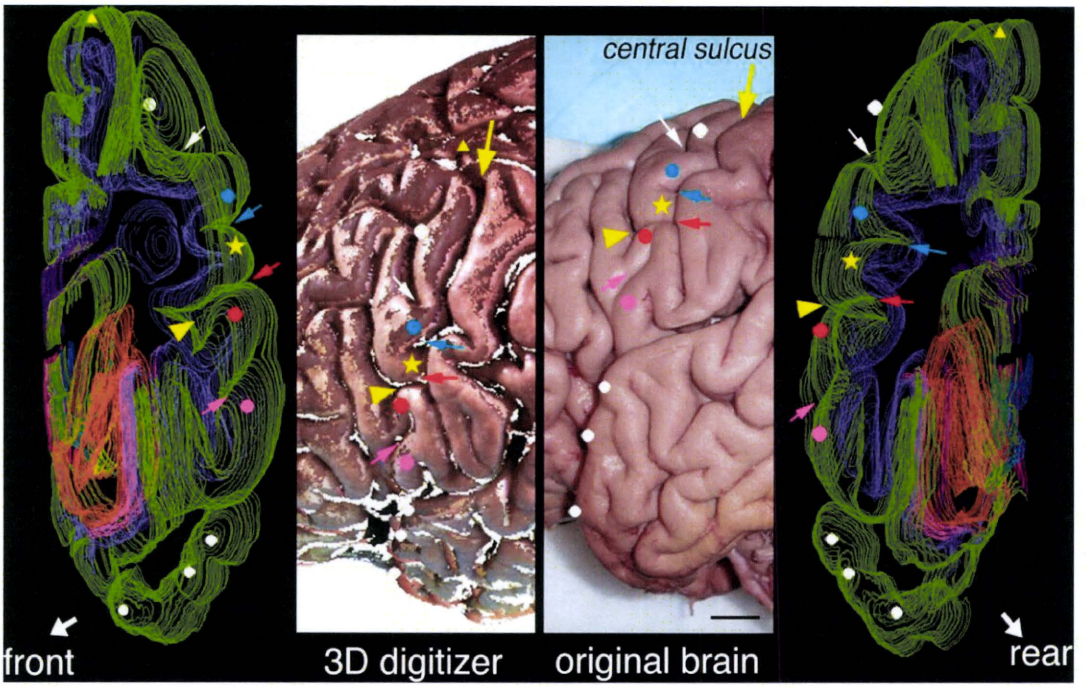

Fig. 6. Correspondence of the reconstructions and 3D digitizer model with the original brain. The same sulci and gyri are shown by the same arrows and symbols, respectively. Yellow large arrows indicate the central sulcus. Reconstructions shown on both sides of the figure are the images viewed from different angles. Yellow triangles on top of the reconstructions are located in the dorsal part of the precentral gyrus and correspond to the site of light micrograph in Fig. 3A. Scale bar: 1 cm. (For interpretation of the references to color in this figure legend, the reader is referred to the web version of the article.)

The material used was not processed systematically for immunohistochemistry, as the conventional procedures for gross anatomy course at our institute are not necessarily appropriate for it. However, specific immunostaining was obtained for methionin-enkephalin in our preliminary study on a large specimen containing both the dorsal and ventral striatum. The present method will be applicable to immunohistochemical examinations of various neuroactive substances as far as the condition of the tissue is well preserved, and in that case immunohistochemistry will be possible over the large-sized nuclei of the human brain.

There might be some arguments on the possible postmortem change in the gross morphology of the brain. Deformity of this type will more or less happen in conventional autopsy cases, because in pathological examinations the untreated, soft and fragile brain is removed from the skull and is fixed thereafter by immersing it in a solution for a long period. By contrast, the postmortem deformity in the present method is thought to be minimum, as the structure of the whole body was preserved by perfusion of the fixative from the femoral artery and tissues were thus hardened with formalin *in situ*. As a result the gross morphology of the whole cadaver including the brain was well preserved when dissection.

Obtained materials can be scanned and stored as digital image files at the light microscopic level that can never be provided by CT or MRI data. The image database can be used for three-dimensional reconstructions of the human brain and further for development of histological reference maps applicable to modern neurosurgical treatments. The deep brain stimulation in particular is now targeting more confined regions for broader disease spectrum than currently executed (Miyagi et al., 2009), thus requiring more precise knowledge on finer anatomy (Miyagi et al., 2007). The present method will be able to provide the database for reconstructing the digitized brain of the human that can be applied to brains of individual patients by using the best algorism of non-rigid deformation (Morooka et al., 2007).

Acknowledgements

The authors wish to thank Takehiro Koya, Megumi Ueguchi, Mai Koga, Ayumi Ishi and Tsubasa Masuoka for their excellent technical assistance. This study was supported by Kyushu University Interdisciplinary Program in Education and Projects in Research Development (P&P), Suzuki Memorial Foundation, and JPSP Kakenhi Grant-in-Aid for Scientific Research (C) 1591873.

Appendix A. Supplementary data

Supplementary data associated with this article can be found, in the online version, at doi:10.1016/j.neures.2010.03.005.

References

Caminiti, R., Ghaziri, H., Galuske, R., Hof, P.R., Innocenti, G.M., 2009. Evolution amplified processing with temporally dispersed slow neuronal connectivity in primates. Proc. Natl. Acad. Sci. U.S.A. 106, 19551–19556.

Foxman, B.T., Oppenheim, J., Petito, C.K., Gazzaniga, M.S., 1986. Proportional anterior commissure area in humans and monkeys. Neurology 36, 1513–1517.

Fukuda, T., Nakano, S., Yoshiya, I., Hashimoto, P.H., 1993. Persistent degenerative state of non-pyramidal neurons in the CA1 region of the gerbil hippocampus following transient forebrain ischemia. Neuroscience 53, 23–38.

Miyagi, Y., Shima, F., Sasaki, T., 2007. Brain shift: an error factor during implantation of deep brain stimulation electrodes. J. Neurosurg. 107, 989–997.

Miyagi, Y., Okamoto, T., Tobimatsu, S., Nakanishi, Y., Aihara, K., Hashiguchi, K., Murakami, N., Yoshida, F., Samura, K., Nagata, S., Sasaki, T., 2009. Spectral analysis of field potential recordings by deep brain stimulation electrode for localization of subthalamic nucleus in patients of Parkinson's syndrome. Stereotac. Func. Neurosurg. 87, 211–218.

Morooka, K., Matsui, S., Nagahashi, H., 2007. Self-organizing deformable model for mapping 3D object onto arbitrary target surface. In: Proceedings of the 6th International Conference on 3-D Digital Imaging and Modeling, pp. 193–200.

Morooka, K., Miyagi, Y., Fukuda, T., Okamoto, T., Hayami, T., Chen, X., Sunagawa, K., Tobimatsu, S., Yoshiura, T., Hashizume, M., 2009. Digital brain atlas for safe and accurate stereotactic neurosurgery. In: Abstract in 6th Annual World Congress for Brain Mapping and Image Guided Therapy.

A02-9 Construction of Brain Simulator System for Computer-aided Diagnosis and Therapy: Progress Overview FY2010

Yasushi Miyagi [#1], Ken'ichi Morooka [*2], Takaichi Fukuda [§3], Tsuyoshi Okamoto [#4], Kenji Sunagawa [#5]

[#] *Graduate School of Medical Sciences, Kyushu University*
3-1-1 Maidashi, Higashi-Ku, Fukuoka 812-8582, Japan
[1] yamiyagi@digital.med.kyushu-u.ac.jp
[4] okamoto@digital.med.kyushu-u.ac.jp
[5] sunagawa@cardiol.med.kyushu-u.ac.jp

[*] *Graduate School of Information Science and Electrical Engineering, Kyushu University*
744 Motooka, Nishi-Ku, Fukuoka 819-0395, Japan
[2] morooka@ait.kyushu-u.ac.jp

[§] *Department of Anatomy and Neurobiology, Faculty of Life Sciences, Kumamoto University*
1-1-1 Honjo, Kumamoto 860-8556, Japan
[3] tfukuda@kumamoto-u.ac.jp

***Abstract*—The purpose of this paper is to construct a brain simulator for the establishment of safe and accurate functional neurosurgery. Classical human brain atlases lack in universality and 3D-consistancy because of limited number of human brain materials. Using the digital imaging technique and micro-slicing technique, we have developed a novel method to construct the stereotactic brain atlas of human with the successful preservation of both histological quality and stereotactic accuracy. This method enables the stereotactic brain atlas of the specific populations, such as race and disease, and enables tailor-made neurosurgery. Japanese specialized for functional neurosurgery. In this project, we are going to extend the stereotactic brain atlas into the universal and multipurpose brain simulator. The future role of this brain simulator is to work as a knowledge database in relation to the local structure of the human brain and as a core of computational anatomy in neuroscience.**

I. Background

The increase in stereotactic and functional neurosurgery in Japan has urged us to develop an ideal human brain atlas, especially specified to the Japanese. An ideal brain atlas must provide the universal coordinates of standard healthy brain, however, the morphology of human brain inevitably contains considerable inter-individual variety while the classical human brain atlases have been made from limited number of brain materials [1], [2]. Only a simple magnification in each axis is a rationale to apply an atlas to individual patient (Fig.1), apart from tailor-made surgery. Probabilistic functional atlas [3] includes a postoperative surgical result of large population and probable distributions of only three functional targets (internal segment of globus pallidus, subthalamic nucleus and nucleus ventrointermedius of thalamus), which may suggest a tentative coordinates for stereotactic functional neurosurgery. Actually, however, what we need is a clear boundary of functional target structure but not probability in individual clinical practice. The tailor-made neurosurgery can be achieved in a true sense, only when the atlas could be deformed to fit to the individual brain. Furthermore, stereotactic functional neurosurgery is increasingly being introduced to wider range of neural circuit disorders; therefore, all basal ganglia nuclei or neural fibers can be a functional target in future and we need to prepare the basis of further development of stereotactic and functional neurosurgery. Lastly, not only macroscopic, but also a microscopic histology is prerequisite for the value of brain atlas in neuroscience research.

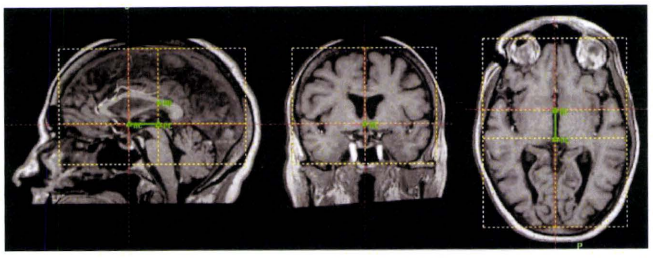

Fig. 1. A simple orthogonal magnification of classical brain atlas

Because a large and soft organ such as human brain is subject to a mechanical deformation, the production of stereotactic human brain atlases is still time-consuming and needs special instruments, environments, manpower and skills. To achieve both the 3D-consistency and high histological quality for stereotactic human brain atlases, we have established a novel method using a formalin-fixed cadaver brain of the Japanese, blade-oscillation microslicer and information engineering technique [4]. This method enabled the reconstruction of histological sections of human brain with the 3D-consistency excellent enough to make the stereotactic atlases of human brain, as well as the successful preservation of original macroscopic shape and microscopic features, such

as cytoarchitecture [5]. We have extended this method in order to construct a brain simulator for safe and accurate functional neurosurgery. Neuroscience researches, such as neural circuit simulator or computational modelling, will further develop explosively when they have the organic link to the neuroanatomical knowledge database made by Brain simulator as a platform.

II. Purpose

Development of multimodal brain atlas is one of top agendas in neuroscience research [6]. The purpose of this project is to construct a brain simulator for the establishment of safe and accurate functional neurosurgery. In this sense, the following specific goals are raised in each step towards the construction of brain simulator.

1. To promote efficiency in constructing histological atlas from the whole brain from a Japanese
2. To develop non-rigid deformation of brain atlas tailored to individual patient
3. To promote data collection form MR images and the extraction of the deformation parameters
4. To register the functional data in each coordinate of the atlas
5. To simulate the functional and mechanical response to trauma, edema, surgical maneuver.

III. Plan

A. Construction of Histological Brain Atlas

We have applied a digital imaging technique and blade-oscillation microslicer to the construction of stereotactic histological brain atlas of human. Namely, the surface of a cadaver brain of a Japanese male was scanned by non-contact 3D-digitizer (VIVID910, Konica Minolta Inc., Japan) and integrated in one surface model as a digital data [4].

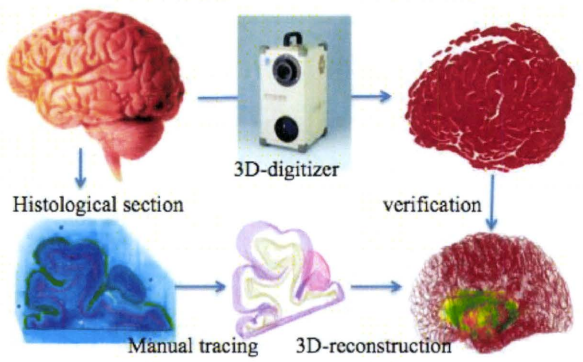

Fig. 2. A method of 3D-reconstruction of the histological sections of the Japanese male brain

The brain was divided into coronal blocks perpendicular to the intercommissural line by brain-cutting machine (VC-600, Meiko Medical Ltd., Japan) and sliced into histological sections using blade-oscillation microslicer (DTK-3000W, Dosaka-EM, Japan).

Histological sections were stained with Nissl- and Myelin-stain and they were scanned into bitmap format. After the four fiducial markers in gelatin frame were used for coregistration of section images slice to slice within a block, the surface contours, ventricles and major subcortical neural structures in the images were manually traced using 3D neuron reconstruction software, Neurolucida (MicroBrightField, Inc., USA) (Fig.2) [4],[5].

B. Construction of Computational Brain Model

Multiple T1-weighted MR brain images of normal volunteers of various ages (control) and movement disorders (dystonia or Parkinson's disease) are separately converted into brain models and the boundaries of subcortical structures visible on MR, such as white mater, ventricle, caudate and putamen, are manually traced using Neurolucida and reconstructed into one 3D model. In control and disease group (dystonia and Parkinson's disease), the regional atrophy ratios are calculated and registered to the coordinates of histological brain atlas. The regional atrophy ratio will be later used for the parameters of individual deformation of standard histological brain atlas. Furthermore, the material data and functional data reported elsewhere in the literatures will be registered to the coordinates.

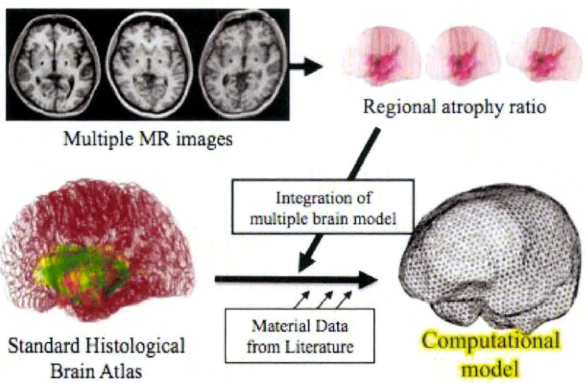

Fig. 3. A method of construction of computational brain model

C. Construction of Brain Simulator

Once a computational brain model is established, the model can be extended to work in almost all fields of neuroscience. To use a model as a simulator, the following 4 functions should be prepared; 1) tailor-made deformation to fit individual brain image, 2) anatomical platform for neural circuit model to predict a therapy effect, 3) navigation system for neurosurgery to overcome intraoperative deformation, 4) registration of functional data as an updatable storage. These functions enable us to use computational brain model directly

in clinical practice of neurology, medical education, neuroscience research and industrial technology.

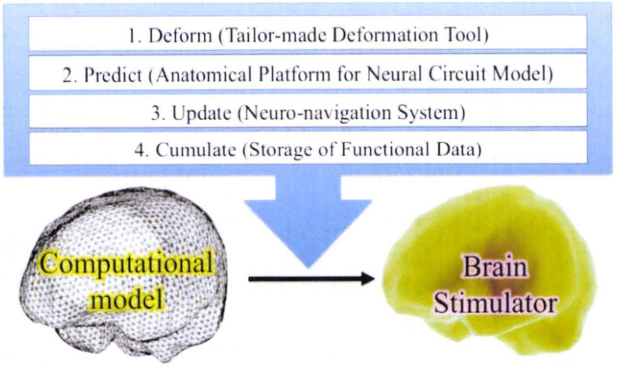

Fig. 4. Brain simulator as a computational brain model with 4 functions

IV. Achievements in 2010

A. Construction of Histological Brain Atlas

A whole brain from the cadaver, 59 year-old male who died of acute deterioration (2 days) of chronic obstructive pulmonary disease was obtained. Before its use in this study, the body was perfused with 10% formalin through femoral artery within 3 hours after death and further immersed in alcohol and used for the gross anatomy practical course of medical students in Kyushu University. After a few years of immersion, the brain was carefully extracted and used in the practical course of anatomical education and stored in 10% formalin. Gross observation in the formalin-fixed brain detected minimal senile atrophy and there was no pathological lesion in the cutting edge of every block.

The hemisphere embedded in agar was further cut into 1 cm-thick block, perpendicular to intercommissural line. The blocks were made as small as it can be mounted on the tissue holder (70x70mm) of blade-oscillation micro-slicer.

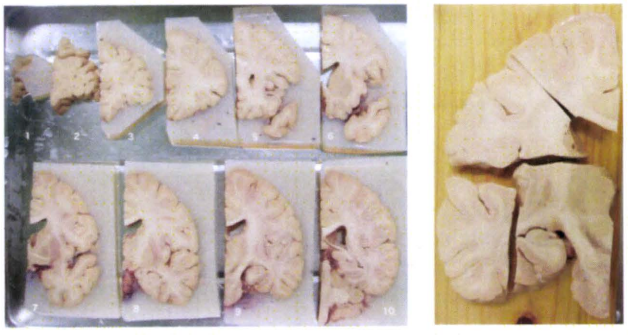

Fig. 5. Coronal block of hemisphere from cadaver

The histological sections with Nissl stain were scanned into bitmap format and the neural structures were manually traced using Neurolucida.

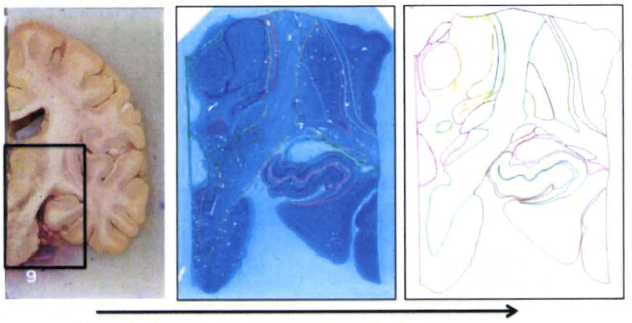

Fig. 6. Manual tracing of the neural structure

B. Digitalization of Classical Atlas

Manual tracing of the neural structures is a considerably time-consuming work; therefore, in order to promote efficiency in manual tracing of neural structures, the classical brain atlas made by Mai et al. [7] was digitalized as a reference. This digitalized model can be cut in an arbitrary section and superimposed on the histological sections, when identifying a region-specific neurons and cytoarchitecture.

C. Data collection of 3D-MRI of normal brain

High-resolution T1-weighted MR images of brain in healthy volunteers were collected. So far, 19 MR images (20-29 yr, 3 males and 1 female; 30-39 yr, 2 females; 40-49 yr, 2 males and 1 female; 50-59 yr, 5 males; 60-69 yr, 4 males and 1 female) were collected.

Using Neurolucida, visible neural structures on T1-MR images were manually traced and being reconstructed. These 3D models will be used for non-rigid deformation and collection of regional atrophy ratio for normal aging and disease population.

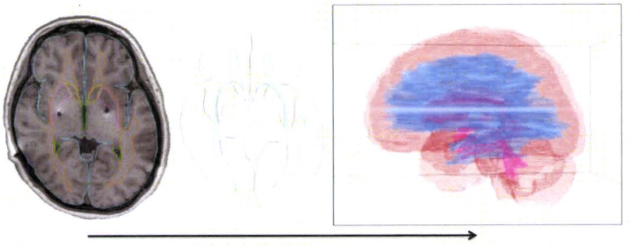

Fig. 7. Manual tracing of the boundaries of visible neural structure

D. 2D-deformation Program

By use of self-organizing deformable model by Morooka et al. [8], the programming for non-rigid deformation of brain atlas is now on-going study with 2D model (a plane including intercommissural line). Once the 2D-deformation method is established, the program will be extended in 3D-model. The histological brain atlas will be deformed to fit individual brain MR images as a tailor-made brain atlas.

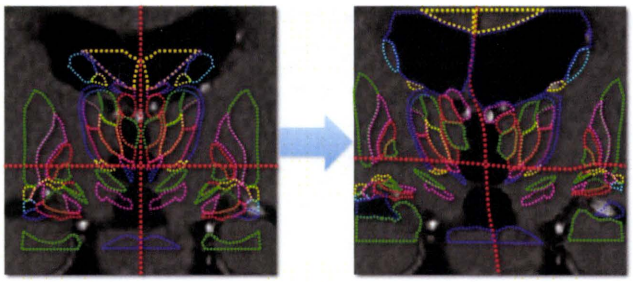

Fig. 8. A goal of non-rigid 3D-deformation for tailor-made atlas

V. Future direction in 2011

The computational brain model is now being constructed. In each step, the collection of MR images, the conversion to 3D-model and non-rigid deformation are the most time-consuming and essential determinants in this project. Further revolution to "Brain Simulator" will be achieved when 4 important functions; tailor-made brain atlas (deform), simulation of therapy (predict), intraoperative navigation (update), updatable knowledge database (cumulate).

Acknowledgment

We are grateful to Mr. T. Koya, Ms. M. Ueguchi, Ms. M. Koga, Ms. A. Ishii, Ms. S. Noda, Ms. S. Sasaki, Ms. N. Fukuyoshi, Ms. K. Fukuda for their important contributions to this project.

References

[1] G. Schaltenbrand and W. Wahren, *Atlas for stereotaxy of the human brain.* Thieme, Stuttgart, 1977.

[2] J. Talairach and P. Tournoux, *Co-planner stereotactic atlas of the human brain.* Thieme, New York, 1988.

[3] W.L. Nowinski and A. Thirunavuukarasuu: *The Cerefy Clinical Brain Atlas on CD-ROM.* New York, Thieme, 2004.

[4] K. Morooka, T. Fukuda and Y. Miyagi, T. Hayami, T. Okamoto, X. Chen, "3D Human brain modeling for constructing Japanese brain database," *Fourth International Workshop on Medical Imaging and Augmented Reality*, 2008.

[5] T. Fukuda, K. Morooka and Y. Miyagi, "A simple but accurate method for histological reconstruction of the large-sized brain tissue of the human that is applicable to construction of digitized brain database," *Neurosci Res* 67(3):260-265, 2010.

[6] A.W. Toga, P.M. Thompson, S. Mori, K. Amunts and K. Zilles, "Towards multimodal atlases of the human brain," *Nature Rev* 7:952-966, 2006.

[7] J.K. Mai, G. Paxinos and T. Voss, *Atlas of the Human Brain, Third Edition. Academic Press, 2007*

[8] K. Morooka, S. Matsui and H. Nagahashi "Self-organizing Deformable Model for mapping 3D Object Model onto Arbitrary Target Surface", *The 6th International Conference on 3-D Digital Imaging and Modeling*, pp.193-200, 2007

List of accepted and published papers since 1st April 2010

[9] Y. Miyagi, T. Fukuda, K. Morooka, K. Chen, T. Hayami, T. Okamoto, K. Sunagawa, S. Tobimatsu and T. Yoshiura, "Application of digital imaging technique for the construction of stereotactic human brain atlas," *Functional Neurosurg* 49(2):136-141, 2010.

Case Report

Stereotactic and Functional Neurosurgery

Stereotact Funct Neurosurg 2010;88:259–263
DOI: 10.1159/000315464

Received: July 30, 2009
Accepted after revision: March 14, 2010
Published online: June 8, 2010

Thalamic Deep Brain Stimulation for the Treatment of Action Myoclonus Caused by Perinatal Anoxia

Kazutaka Kobayashi[a, b] Yoichi Katayama[a, b] Toshiharu Otaka[a, b]
Toshiki Obuchi[a, b] Toshikazu Kano[a, b] Takafumi Nagaoka[a, b] Masahiko Kasai[a]
Hideki Oshima[a, b] Chikashi Fukaya[a, b] Takamitsu Yamamoto[a, b]

[a]Division of Neurosurgery, Department of Neurological Surgery, and [b]Division of Applied System Neuroscience, Department of Advanced Medical Science, Nihon University School of Medicine, Tokyo, Japan

Key Words
Myoclonus · Deep brain stimulation · Thalamus · Perinatal anoxia

Abstract
Background: Perinatal anoxia rarely causes myoclonus as the main neurologic abnormality. The exact neuronal mechanism underlying myoclonus induced by perinatal anoxia remains unknown. Some studies have indicated that the development of involuntary movements may be related to the maturation of the thalamus after birth. ***Objectives and Methods:*** Here, we describe the first case of a patient who developed action myoclonus after experiencing perinatal anoxia and was successfully treated by chronic deep brain stimulation (DBS) of the thalamus (thalamic DBS). ***Results and Conclusion:*** The effectiveness of chronic thalamic DBS in this patient supports the concept of involvement of the thalamus in postperinatal anoxic myoclonus.

Introduction

Myoclonus is rarely the main neurologic sequela of perinatal anoxia [1–3]; it is more commonly observed after brain anoxia in adults [1–3]. Deep brain stimulation (DBS) of the thalamus (thalamic DBS) is effective for the treatment of tremors [4–13]. Furthermore, thalamic DBS has been reported to effectively control various other involuntary movements such as hemiballismus [8, 14], writer's cramp [15] (which is a type of dystonia) and chorea associated with a case of cerebral palsy [16]. This treatment has also been found to ameliorate myoclonic symptoms in patients with inherited myoclonus dystonia syndrome [17–19]. However, the effectiveness of DBS for the treatment of myoclonus induced by perinatal anoxia has not yet been studied. We report here the case of a patient who developed action myoclonus as a result of perinatal anoxia and was successfully treated by thalamic DBS.

Case Report

Patient History

A 36-year-old right-handed man presented with marked aggravation of involuntary movements. The patient had a history of perinatal hypoxia and was diagnosed as having floppy infant syn-

KARGER

Fax +41 61 306 12 34
E-Mail karger@karger.ch
www.karger.com

1011–6125/10/0884–0259$26.00/0

Accessible online at:
www.karger.com/sfn

Kazutaka Kobayashi, MD, PhD
Department of Neurological Surgery, Nihon University School of Medicine
30-1 Oyaguchi Kamimachi
Itabashi-ku, Tokyo 173-8610 (Japan)
Tel. +81 33 972 8111, Fax +81 33 554 0425, E-Mail kitta@med.nihon-u.ac.jp

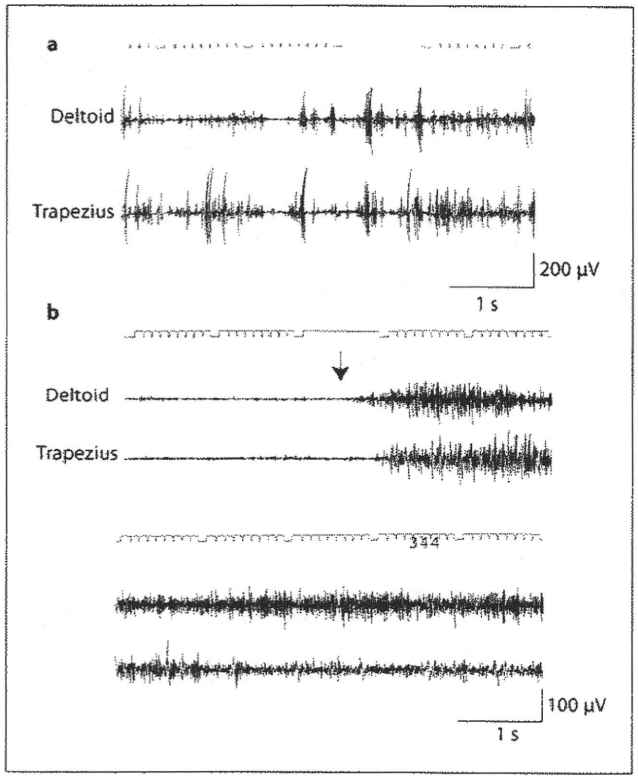

Fig. 1. Surface electromyography (EMG) of the deltoid and trapezius in the present patient. **a** Before surgery; recording of the patient attempting to hold his left arm in front of him. **b** After surgery; recording during thalamic stimulation. The arrow indicates the point at which the patient started to hold his left arm out in front of him. (Note: the EMG amplitude scale differs between **a** and **b**.)

drome at birth. He had an unsteady gait due to hypotonia of the muscles of the lower limbs and required an orthotic for walking between the ages of 12 and 18 months. He was diagnosed as having cerebral palsy at 18 months of age. He developed slight involuntary movements of both his upper limbs at 4 years of age. At 13 years of age, these involuntary movements became markedly aggravated; they subsequently progressed to jerky movements and have worsened steadily with advancing age. He has undergone treatment with several drugs, without any obvious effect. He was therefore finally referred to our hospital for DBS surgery at 36 years of age.

On examination, jerky movements of both upper limbs, mainly the proximal limbs, were observed, with no cerebellar signs such as hypotonia or hand ataxia. The involuntary movements appeared occasionally at rest. The finger-to-nose test aggravated the involuntary movements without ataxia. The involuntary movements were stereotyped. Electromyography using surface electrodes revealed irregular and repetitive burst discharges when the patient performed any action, particularly elevation of the arm or holding a cup (fig. 1a). The item of severity of myoclonus with action of the arm on the Unified Myoclonus Rating Scale (UMRS) [20] was employed to evaluate the action myoclonus. This item is scored as the product of scores for the frequency and amplitude of myoclonus with action. The frequency of myoclonus is scored as follows: no jerks per 10 s, 0; ≤1 jerk per 10 s, 1; 2 or 3 jerks per 10 s, 2; 4–9 jerks per 10 s, 3; ≥10 jerks per 10 s, 4. The amplitude of the worst myoclonus seen on finger-to-nose testing is scored using the following procedure: ask the patient to hold both arms forward with the palms down for 10 s, then ask the patient to extend both wrists for 10 s, then perform the finger-to-nose test 4 times and finally, ask the patient to finish by leaving his finger on his nose for 10 s. The movement is scored as follows: zero, 0; trace movement only, 1; small-amplitude jerks, easily visible (<25% of maximum possible movement), 2; moderate-amplitude jerks (25–75% of maximum possible movement), 3; large-amplitude jerks (near maximum movement), 4. The score for the severity of myoclonus with action of the arm on the UMRS was 12 for the left arm and 9 for the right arm.

Magnetic resonance (MR) imaging of the brain revealed slight brain atrophy, without any other abnormalities. The involuntary movements improved at rest and disappeared during sleep. There was no known family history of movement disorder or other neurological disease. We made plans to conduct surgery on the patient for implantation of a DBS electrode to treat the myoclonus, and obtained the informed consent of the patient and his family. We did not schedule the performance of bilateral surgery at one time because we needed to confirm the effectiveness of DBS for the patient. We therefore planned the introduction of an electrode in the right thalamus first, since the involuntary movements of the left hand were worse than those of the right hand.

Surgical Procedure

The surgical procedure was planned using MR images. Following the administration of a local anesthetic, a Leksell G head frame (Elekta Instruments AB) was applied to the patient's head. The anterior commissure (AC) and posterior commissure (PC) were identified using Leksell SurgiPlan® (Elekta Instruments AB), a customized software program for functional stereotaxy. An X-ray indicator (Elekta Instruments AB) was also employed to identify the AC and PC on plain X-ray films. A burr hole was made approximately 2.0 cm anterior to the coronal suture and approximately 2.5 cm lateral to the midline. Extracellular single- and multiunit recordings were obtained using a semimicroelectrode (0.4 MΩ). With the intention of identifying the anterior border of the nucleus ventrocaudalis (Vc), which constitutes the nucleus ventralis intermedius (Vim)-Vc border, we directed the first trajectory of the semimicroelectrode utilized for extracellular unit recording toward the anterior aspect of the PC in lateral view and at the level of the AC-PC line and 14.5 mm lateral to the midline. Neuronal activity was also fed into an audiospeaker. The neuronal activity was examined under various conditions such as somatic sensory stimulation and active movements. Neurons that were activated in response to somatic sensory stimulation, that is, in response to passive joint movements of the contralateral limb without a response in skin deformation caused by the stimuli, were classified as (1) deep sensory cells; and neurons that responded to light touch on the skin of the face and contralateral limbs were classified as (2) cutaneous sensory cells. The Vim-Vc border was defined physiologically as the anterior-most neurons along a trajectory which was mapped such that >50% of the neu-

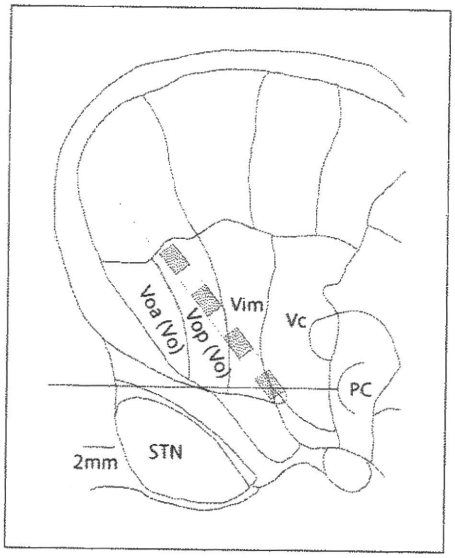

Fig. 2. Anatomical relationship between the thalamic nucleus and DBS electrode. **a** A 14.5-mm lateral section from the Schaltenbrand-Wahren human brain atlas with the AC-PC length stretched to fit the coordinates obtained from the patient's stereotactic magnetic resonance images. STN = Subthalamic nucleus; Voa = nucleus ventralis oralis anterior; Vop = nucleus ventralis oralis posterior.

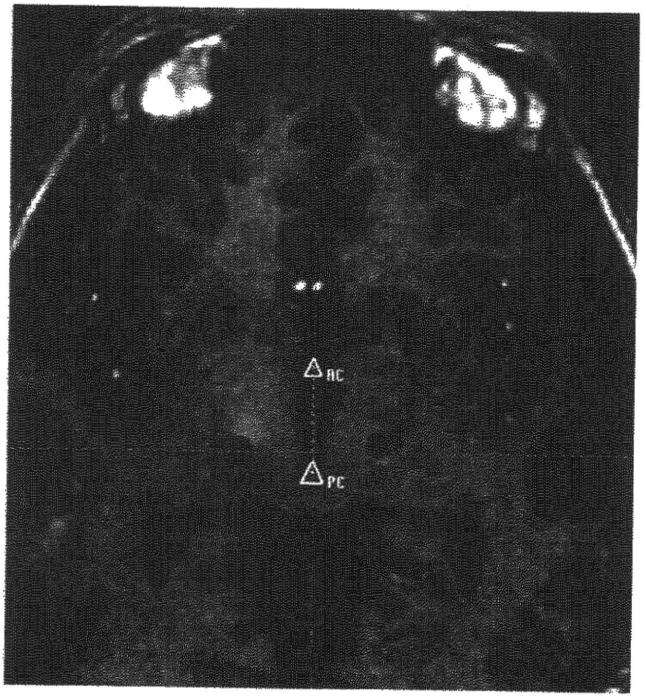

Fig. 3. Location of bilateral DBS electrodes on magnetic resonance (MR) imaging. Postoperative T_1-weighted axial MR imaging of the brain revealed the lead locations at the level of the AC-PC commissural plane. The leads are visualized as dark circular spots in the brain parenchyma.

rons located posterior to the trajectory were either deep or cutaneous sensory neurons [21]. On the basis of observations made during our initial trajectory assessment, the Vim-Vc border was identified as a vertical line approximately 3 mm anterior to the PC. This identification was consistent with the Vim-Vc border determined based on the Schaltenbrand-Wahren atlas. The second trajectory of the semimicroelectrode was directed toward a position on the Vim-Vc border at the level of the AC-PC line, 14.5 mm lateral to the midline. The target was approached through the burr hole at an angle of 52° to the horizontal plane of the AC-PC line. Subsequently, the DBS electrode (model 3387; Medtronic Inc., Minn., USA) was implanted through the second trajectory using stereotactic instruments, and a test stimulation was conducted with the DBS electrode in place. This electrode has 4 contacts that are numbered sequentially from 0 to 3, with the most distal contact being 0 and the most proximal contact being 3. Each contact is 1.5 mm long, and the contacts are spaced 1.5 mm apart. The DBS electrode was implanted to cover a wide region of the thalamus, including not only the Vim but also the nucleus ventralis oralis (Vo).

Contact 0 was located at the Vim-Vc border; contact 1 in the central part of the Vim, and contacts 2 and 3 within the Vo (fig. 2). Test stimulations were performed for 4 days after completion of the procedure to confirm myoclonus suppression (fig. 1b). The stimulations showed that satisfactory control of the involuntary movements had been achieved. Therefore, under general anesthesia, an internal pulse generator (Soletra; Medtronic) was placed in an infraclavicular pocket and connected subcutaneously to the DBS lead. After 2 weeks, another DBS electrode was implanted into the left Vo/Vim, and a pulse generator was also implanted using the method described above (fig. 3).

Postoperative Outcome

After the operations, we assessed the most effective combination of contacts of the electrode at a frequency of 135 Hz and a pulse width of 0.21 ms. The voltage of stimulation was increased to an upper limit where such adverse effects as paresthesia began to appear. The effect of stimulation was evaluated with blinded contact combinations.

The following combinations stimulated mainly the Vim (fig. 2): contact 0 as the anode (+) and contact 1 as the cathode (–), contact 1 as the cathode (–) and contact 2 as the anode (+), and monopolar stimulation using contact 1 as the cathode (–); these combinations had some effect on the myoclonus. However, the strongest effect was achieved when contact 1 was the cathode (–) and contact 3 was the anode (+); this combination activated a wide area extending from the Vo to the Vim. When contact 0 located in the Vc was used as the cathode (–), paresthesia was evoked by a low intensity of stimulation. The optimal combinations were the same on both sides. At the 24-month follow-up, the item of severity of myoclonus with action of the arm on the UMRS score was reduced from 12/16 to 2/16 for the left arm and from 9/16 to 2/16 for the right arm (table 1).

Table 1. Efficacy of thalamic DBS for myoclonus

Severity of myoclonus with action of the arm on the UMRS	Left arm		Right arm	
	before surgery	after surgery	before surgery	after surgery
Total score (frequency × amplitude)	12	2	9	2
Frequency	4	2	3	2
Amplitude	3	1	3	1

The combination of electrode contacts used was as follows: contact 1 as the cathode (–) and contact 3 as the anode (+).

Scores are between 0 (best) and 4 (worst) for frequency and amplitude and between 0 (best) and 16 (worst) for total.

Discussion

Perinatal anoxia can, on rare occasions, induce myoclonus as the main neurologic abnormality [1–3]. The detailed pathophysiology of postperinatal anoxic myoclonus remains unknown. Some reports have suggested that the symptoms of myoclonus after perinatal anoxia of the ascending efferents of the basal ganglia to the thalamus and the thalamocortical pathways are not observed in the first decade of life, despite the development of pathological lesions specific to these symptoms [22, 23]. Moreover, Sugama and Kusano [3] suggested that the development of movement disorder due to perinatal anoxia may be related to the maturation of the thalamus after birth. Our patient could thus have been in a thalamotomy-like state during the infantile period because of the immaturity of the thalamus. With advancing age, various involuntary movements develop after the maturation of the thalamus [3]. The effectiveness of chronic thalamic DBS in our patient may provide support for the concept of involvement of the thalamus in postperinatal anoxic myoclonus.

Recently, it has been reported that thalamic DBS ameliorated myoclonus in a patient with myoclonus dystonia syndrome; this patient did not have a history of perinatal anoxia [17–19]. The optimal site for thalamic DBS remains to be determined. Although the exact mechanisms underlying myoclonus are not understood, a study on monkeys has indicated that dysfunction of the Vim in the thalamus may play a role in the generation of myoclonic jerks [24]. In our patient, however, the most effective stimulation site covered a wide area that included the Vo in addition to the Vim. Tremor suppression is generally attributed to stimulation of the Vim but has been reported to follow stimulation of the Vo [25] or a wide area centered on the Vim and including the Vo [26]. In the large series of cases presented by Benabid et al. [4], the optimal tremor control site was located 4–8 mm anterior to the PC and 0–2 mm superior to the AC-PC line. From these coordinates, we infer that the areas stimulated by spread of the electrical current included not only the Vim but also the Vo [27]. Consistent with our findings, Trottenberg et al. [19] suggested that the effect of thalamic stimulation on myoclonus in myoclonus dystonia syndrome may be attributable to electrophysiological ablation of the Vo and Vim or nearby fiber systems.

Conclusions

We successfully treated a patient with severe action myoclonus due to perinatal anoxia by thalamic DBS. Such thalamic DBS may offer an effective and safe treatment modality for intractable postperinatal anoxic myoclonus.

References

1 Obeso JA, Lang AE, Rothwell JC, Marsden CD: Postanoxic symptomatic oscillatory myoclonus. Neurology 1983;33:240–243.

2 Rondot P, Said G, Ferrey G: Volitional hyperkinesia: electrological study: classification. Rev Neurol (Paris) 1972;126:415–426.

3 Sugama S, Kusano K: A case of dyskinetic cerebral palsy resembling post-anoxic action myoclonus. Brain Dev 1995;17:210–212.

4 Benabid AL, Pollak P, Gao D, Hoffmann D, Limousin P, Gay E, Payen I, Benazzouz A: Chronic electrical stimulation of the ventralis intermedius nucleus of the thalamus as a treatment of movement disorders. J Neurosurg 1996;84:203–214.

5 Benabid AL, Pollak P, Gervason C, Hoffmann D, Gao DM, Hommel M, Perret JE, de Rougemont J: Long-term suppression of tremor by chronic stimulation of the ventral intermediate thalamic nucleus. Lancet 1991; 337:403–406.

6 Blond S, Caparros-Lefebvre D, Parker F, Assaker R, Petit H, Guieu JD, Christiaens JL: Control of tremor and involuntary movement disorders by chronic stereotactic stimulation of the ventral intermediate thalamic nucleus. J Neurosurg 1992;77:62–68.

7 Caparros-Lefebvre D, Blond S, Vermersch P, Pecheux N, Guieu JD, Petit H: Chronic thalamic stimulation improves tremor and levodopa-induced dyskinesias in Parkinson's disease. J Neurol Neurosurg Psychiatry 1993; 56:268–273.

8 Katayama Y, Fukaya C, Yamamoto T: Control of poststroke involuntary and voluntary movement disorders with deep brain or epidural cortical stimulation. Stereotact Funct Neurosurg 1997;69:73–79.
9 Koller WC, Lyons KE, Wilkinson SB, Troster AI, Pahwa R: Long-term safety and efficacy of unilateral deep brain stimulation of the thalamus in essential tremor. Mov Disord 2001;16:464–468.
10 Limousin P, Speelman JD, Gielen F, Janssens M: Multicentre European study of thalamic stimulation in parkinsonian and essential tremor. J Neurol Neurosurg Psychiatry 1999; 66:289–296.
11 Nguyen JP, Degos JD: Thalamic stimulation and proximal tremor: a specific target in the nucleus ventrointermedius thalami. Arch Neurol 1993;50:498–500.
12 Yamamoto T, Katayama Y, Kano T, Kobayashi K, Oshima H, Fukaya C: Deep brain stimulation for the treatment of parkinsonian, essential, and poststroke tremor: a suitable stimulation method and changes in effective stimulation intensity. J Neurosurg 2004;101: 201–209.
13 Yamamoto T, Katayama Y, Fukaya C, Oshima H, Kasai M, Kobayashi K: New method of deep brain stimulation therapy with two electrodes implanted in parallel and side by side. J Neurosurg 2001;95:1075–1078.
14 Katayama Y, Yamamoto T, Kobayashi K, Oshima H, Fukaya C: Deep brain and motor cortex stimulation for post-stroke movement disorders and post-stroke pain. Acta Neurochir Suppl 2003;87:121–123.
15 Fukaya C, Katayama Y, Kano T, Nagaoka T, Kobayashi K, Oshima H, Yamamoto T: Thalamic deep brain stimulation for writer's cramp. J Neurosurg 2007;107:977–982.
16 Thompson TP, Kondziolka D, Albright AL: Thalamic stimulation for choreiform movement disorders in children: report of two cases. J Neurosurg 2000;92:718–721.
17 Kuncel AM, Turner DA, Ozelius LJ, Greene PE, Grill WM, Stacy MA: Myoclonus and tremor response to thalamic deep brain stimulation parameters in a patient with inherited myoclonus-dystonia syndrome. Clin Neurol Neurosurg 2009;111:303–306.
18 Kupsch A, Trottenberg T, Meissner W, Funk T: Neurostimulation of the ventral intermediate thalamic nucleus alleviates hereditary essential myoclonus. J Neurol Neurosurg Psychiatry 1999;67:415–416.
19 Trottenberg T, Meissner W, Kabus C, Arnold G, Funk T, Einhaupl KM, Kupsch A: Neurostimulation of the ventral intermediate thalamic nucleus in inherited myoclonus-dystonia syndrome. Mov Disord 2001;16:769–771.
20 Frucht SJ, Leurgans SE, Hallett M, Fahn S: The unified myoclonus rating scale. Adv Neurol 2002;89:361–376.
21 Hua SE, Lenz FA: Posture-related oscillations in human cerebellar thalamus in essential tremor are enabled by voluntary motor circuits. J Neurophysiol 2005;93:117–127.
22 Segawa M: Pathophysiologies of dystonia and myoclonus: consideration from the standpoint of treatment. Rinsho Shinkeigaku 1995;35:1390–1393.
23 Segawa M: Development of the nigrostriatal dopamine neuron and the pathways in the basal ganglia. Brain Dev 2000;22(suppl 1): S1–S4.
24 Guehl D, Burbaud P, Boraud T, Bioulac B: Bicuculline injections into the rostral and caudal motor thalamus of the monkey induce different types of dystonia. Eur J Neurosci 2000;12:1033–1037.
25 Hassler R, Mundinger F, Riechert T: Stereotaxis in Parkinson Syndrome. Clinical-Anatomical Contributions to Its Pathophysiology. New York, Springer, 1979.
26 Strafella A, Ashby P, Munz M, Dostrovsky JO, Lozano AM, Lang AE: Inhibition of voluntary activity by thalamic stimulation in humans: relevance for the control of tremor. Mov Disord 1997;12:727–737.
27 Starr PA, Vitek JL, Bakay RA: Ablative surgery and deep brain stimulation for Parkinson's disease. Neurosurgery 1998;43:989–1013; discussion 1013–1015.

Neurol Med Chir (Tokyo) 50, 257 ~ 259, 2010

Direct Relief of Levodopa-Induced Dyskinesia by Stimulation in the Area Above the Subthalamic Nucleus in a Patient With Parkinson's Disease

—Case Report—

Yasumasa NISHIKAWA, Kazutaka KOBAYASHI*, Hideki OSHIMA*, Chikashi FUKAYA*, Takamitu YAMAMOTO*, Yoichi KATAYAMA*, Akira OGAWA, and Kuniaki OGASAWARA

*Department of Neurosurgery, Iwate Medical University School of Medicine, Morioka, Iwate; *Division of Applied System Neuroscience, Advanced Medical Research Center, and Department of Neurological Surgery, Nihon University School of Medicine, Tokyo*

Abstract

A 71-year-old woman with a 25-year history of levodopa (LD)-responsive Parkinson's disease (PD) developed on-off motor fluctuation and severe peak dose dyskinesia. She underwent deep brain stimulation of the subthalamic nucleus (STN-DBS). STN-DBS induced attenuation of her cardinal PD symptoms and marked improvement of dyskinesia without reduction of LD dosage perioperatively. STN-DBS thus markedly attenuated the cardinal symptoms of PD. LD-induced dyskinesia can also be controlled via reduction of LD dosage as an indirect effect of STN-DBS. The present case provides evidence of the direct antidyskinetic effect of STN-DBS, and suggests that LD-induced dyskinesia can be inhibited by stimulation in the area above the STN.

Key words: deep brain stimulation of subthalamic nucleus, dyskinesia, Parkinson's disease, antidyskinetic effect, area above subthalamic nucleus

Introduction

Deep brain stimulation of the subthalamic nucleus (STN-DBS) induces attenuation of the cardinal symptoms of Parkinson's disease (PD) during off-periods as well as dopa-induced dyskinesia.[4,9,11-13] Relief of dopa-induced dyskinesia after STN-DBS is believed to depend on postoperative reduction of dopaminergic medication,[6] but STN-DBS may directly decrease dopa-induced dyskinesia.[1,5,10,14] We describe a patient with PD whose dopa-induced dyskinesia improved after STN-DBS.

Case Report

A 71-year-old woman with a 25-year history of levodopa (LD)-responsive PD developed on-off motor fluctuation and peak dose dyskinesia with an LD dose of 500 mg/day. She had suffered fracture of her left femur 11 years previously and had difficulty with ambulation due to contracture of her left lower extremity. About 30–60 minutes after each administration of LD, choreiform dyskinesia developed and persisted for 1 hour. Motor score on the United Parkinson's Disease Rating Scale (UPDRS) motor score was 38 in the off-condition and 28 in the on-condition. Dyskinesia score (six body parts, each scored 0–4, maximum score 24) was 17 in the on-condition.

Bilateral STN-DBS was performed. She continued to receive medication perioperatively, except on the day of the procedure. A tentative target was determined based on magnetic resonance (MR) imaging using human brain atlas software, single- and multi-unit extracellular recording, and microstimulation. Model 3387 DBS electrodes were implanted under microelectrode guidance without complications. The electrodes were directed from the frontal burr hole at an angle of 50° to the horizontal plane.

Postoperative MR imaging demonstrated correct placement of the electrodes (Fig. 1). Two of the four contacts (contacts 0 and 1) were within the STN. Contacts 2 and 3 were located in the area above the STN including the Forel H field and the zona incerta. While receiving the same doses of antiparkinsonian drugs as preoperatively, the patient underwent monopolar stimulation using contacts 0 to 3 as the cathode and a case as the anode. However, dysarthria was observed using all contacts under low amplitude. Then she underwent bipolar stimulation using contacts 0 to 2 as the cathode and contact 3 as the anode. The intensity and frequency of stimulation were 1.8 V and 135 Hz, respectively, and the pulse width was 150 μsec. No adverse effect was observed under these conditions. Using contact 0 or 1 as the cathode, her cardinal Parkinson sym-

Received April 14, 2009; Accepted July 29, 2009

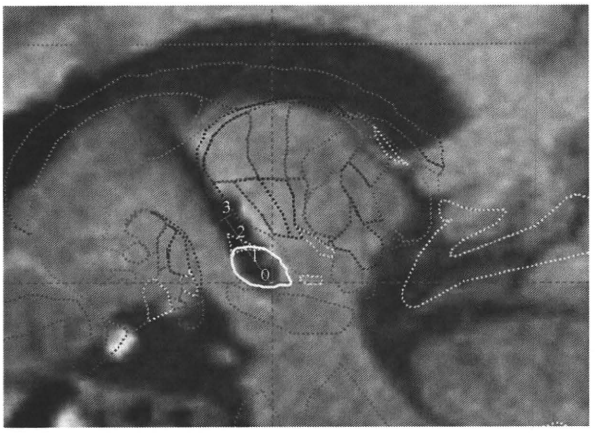

Fig. 1 Postoperative T_1-weighted magnetic resonance image showing contacts placed in the subthalamic nucleus and the area above this nucleus.

Table 1 Correlation between position of the cathode and symptoms under bipolar stimulation

Cathode contact	Rigidity	Tremor	Akinesia	Dyskinesia
0	↓	↓	↓	→
1	↓	↓	↓	→
2	↓	↓	↓	↓↓

Anode was contact 3. →: no change, ↓: decrease, ↓↓: large decrease.

ptoms were improved, although LD-induced dyskinesia remained unchanged. In contrast, using contact 2 as the cathode, both LD-induced dyskinesia and cardinal Parkinson symptoms were markedly attenuated (Table 1). The dose of LD was gradually reduced, and the patient eventually received only dopamine agonist (cabergoline, total dose 1.0 mg/day). The postoperative UPDRS motor score was 27 and the dyskinesia score was 0.

Discussion

The antidyskinetic effect of STN-DBS is due to the postoperative reduction of LD intake.[3,7,15] In contrast, DBS of the globus pallidus internus (GPi) has a direct antidyskinetic effect.[16] GPi-DBS yields significant improvement of LD-induced dyskinesia after surgery without reduction of LD dosage. In our case, bipolar stimulation for STN-DBS using contacts 0 or 1 as the cathode induced attenuation of cardinal PD symptoms but not LD-induced dyskinesia, whereas bipolar stimulation using contact 2 as the cathode induced attenuation of both cardinal PD symptoms and LD-induced dyskinesia without reduction of LD dosage. These findings suggest that stimulation in the area above the STN inhibited LD-induced dyskinesia, consistent with previous findings.[1,5,8,10,14] Pallidothalamic, pallidosubthalamic, and subthalamopallidal fibers are densely distributed in the area above the STN.[10] Furthermore, a study using tracer techniques in the squirrel monkey demonstrated that pallidothalamic fibers originating within the sensorimotor region of the GPi mainly project through the lenticular fasciculus, running through the area above the STN.[2] Stimulation of these fibers may have effects similar to GPi-DBS and thus inhibit dopa-induced dyskinesia.

References

1) Alterman RL, Shils JL, Gudesblatt M, Tagliati M: Immediate and sustained relief of levodopa-induced dyskinesia after dorsal relocation of a deep brain stimulation lead. Case report. *Neurosurg Focus* 17(1): E6, 2004
2) Baron MS, Sidibe M, Delong MR: Course of motor and associative pallidothalamic projections in monkeys. *J Comp Neurol* 429: 490–501, 2001
3) Benabid AL, Benazzouz A, Limousin P, Koudsie A, Krack P, Piallat B, Pollak P: Dyskinesias and the subthalamic nucleus. *Ann Neurol* 47: S189–192, 2000
4) Burchiel KJ, Anderson VC, Favre J, Hammerstad JP: Comparison of pallidal and subthalamic nucleus deep brain stimulation for advanced Parkinson's disease: results of a randomized, blinded pilot study. *Neurosurgery* 45: 1375–1382, 1999
5) Figueiras-Mendez R, Marin-Zarza F, Antonio Molina J, Jimenez-Jimenez FJ, Orti-Pareja M, Magarinos C, Lopez-Pino MA, Martinez V: Subthalamic nucleus stimulation improves directly levodopa induced dyskinesias in Parkinson's disease. *J Neurol Neurosurg Psychiatry* 66: 549–550, 1999
6) Follett KA: Comparison of pallidal and subthalamic deep brain stimulation for the treatment of levodopa-induced dyskinesias. *Neurosurg Focus* 17(1): E3, 2004
7) Fraix V, Pollak P, Van Blercom N, Xie J, Krack P, Koudsie A, Benabid AL: Effect of subthalamic nucleus stimulation on levodopa-induced dyskinesia in Parkinson's disease. *Neurology* 55: 1921–1923, 2000
8) Herzog J, Pinsker M, Wasner M, Steigerwald F, Wailke S, Deuschl G, Volkmann J: Stimulation of subthalamic fibre tracts reduces dyskinesias in STN-DBS. *Mov Disord* 22: 679–684, 2007
9) Katayama Y, Kasai M, Oshima H, Fukaya C, Yamamoto T, Ogawa K, Mizutani T: Subthalamic nucleus stimulation for Parkinson disease: benefits observed in levodopa-intolerant patients. *J Neurosurg* 95: 213–221, 2001
10) Katayama Y, Oshima H, Kano T, Kobayashi K, Fukaya C, Yamamoto T: Direct effect of subthalamic nucleus stimulation on levodopa-induced peak-dose dyskinesia in patients with Parkinson's disease. *Stereotact Funct Neurosurg* 84: 176–179, 2006
11) Krack P, Pollak P, Limousin P, Hoffmann D, Xie J, Benazzouz A, Benabid AL: Subthalamic nucleus or internal pallidal stimulation in young onset Parkinson's disease. *Brain* 121(Pt 3): 451–457, 1998
12) Kumar R, Lozano AM, Kim YJ, Hutchison WD, Sime E, Halket E, Lang AE: Double-blind evaluation of subthalamic nucleus deep brain stimulation in advanced Parkinson's disease. *Neurology* 51: 850–855, 1998
13) Moro E, Scerrati M, Romito LM, Roselli R, Tonali P, Albanese A: Chronic subthalamic nucleus stimulation reduces medication requirements in Parkinson's disease. *Neurology* 53: 85–90, 1999
14) Oshima H, Kobayashi K, Kasai M, Fukaya C, Yamamoto T, Katayama Y: [Effect of subthalamic nucleus stimulation on levodopa-induced dyskinesia]. *Kinoteki No Shinkei Geka* 42: 49–52, 2003 (Jpn, with Eng abstract)

15) Russmann H, Ghika J, Combrement P, Villemure JG, Bogousslavsky J, Burkhard PR, Vingerhoets FJG: L-dopa-induced dyskinesia improvement after STN-DBS depends upon medication reduction. *Neurology* 63: 159–155, 2004
16) Volkmann J, Sturm V, Weiss P, Kappler J, Voges J, Koulousakis A, Lehrke R, Hefter H, Freund HJ: Bilateral high-frequency stimulation of the internal globus pallidus in advanced Parkinson's disease. *Ann Neurol* 44: 953–961, 1998

Address reprint requests to: Yasumasa Nishikawa, M.D., Department of Neurosurgery, Iwate Medical University School of Medicine, 19–1 Uchimaru, Morioka, Iwate 020–8505, Japan.

TABLE 1. *Characteristics of the four operated PD patients with the neck and/or the trunk lateral deviation*

	Present age	Age at PD onset	PD duration on pallidotomy	Years from pallidotomy to symptoms onset	PD duration on symptoms onset	Lesion localization based on MRI
Our pt	61	38	13	4	17	GPi/GPe
Pt 1[a]	72	44	17	8	25	GPi/GPe
Pt 2[a]	63	47	6	9	15	GPi/Internal Capsule
Pt 3[a]	69	43	17	4	21	GPi/GPe/Sella Media
Mean	66.3 ± 5	43 ± 3.7	13.3 ± 5.2	6.3 ± 2.6	19.5 ± 4.4	

[a]Patients 1, 2, and 3 are reported in Ref. 1.

The aggravation of the lateral body deviation by L-dopa could represent a motor asymmetry similar to that observed in rats following a unilateral lesion of the nigrostriatal pathway.[4] In this rotating rat model of Parkinsonism, L-dopa, given weeks after intracerebral injection of the neurotoxin 6-Hydroxydopamine, induces a contralateral body rotation associated with increased ^{3}H-spiroperidol binding in the lesioned striatum.[4] More recent studies[5] have shown that long-term administration of L-dopa to rats lesioned by 6-Hydroxydopamine alters corticostriatal bidirectional synaptic plasticity. As such, it is possible that pallidotomy has altered the local basal ganglia circuitry in our patient, resulting in the L-dopa aggravated motor asymmetry.

In light of the above, we could conclude that contralateral deviation of the head, the neck, and/or the trunk can occur as a delayed adverse event following unilateral pallidotomy. The extension of the primary medial pallidal lesion to other neighboring basal ganglia structures could be the underlying pathogenetic mechanism. In this regard, it is unclear as to why it takes so many years for the deformity to develop following the neurosurgical procedure, when in other acute basal ganglia lesions dystonia occurs immediately or shortly after the destructive event. A long-term postoperational modification of the basal ganglia physiology, perhaps similar to that occurring in the rat model of Parkinsonism in which contralateral rotation requires some time to develop following damage to the nigrostriatal pathway,[4] may be implicated. Since follow-up studies of operated PD patients extend from 1 to 5 years,[6,7] it is not surprising that dystonia is never reported as a postoperative complication of pallidotomy. Follow-up studies of longer duration are needed to reveal the long-term motor consequences of this neurosurgical procedure.

Financial Disclosures: Cleanthe Spanaki has been receiving grants from the Parkinson Disease Foundation and from the Second Operational Program for Education and Initial Vocational Training (EPEAEK II) from the Ministry of Education of Greece. Spyros Zafeiris has nothing to disclose. Andreas Plaitakis has been supported by the European Community and the Ministry of Development/General Secretariat for Research and Technology (Contract grant number: PENED 2003/03ED576) and by the Association for the Advancement of Research and Treatment of Neurologic Disorders of Crete ≪EY ZHN≫.

Authors Roles: Cleanthe Spanaki: Conception and writing of the manuscript; Spiros Zafeiris: Taking care of the patient, providing photographs; Andreas Plaitakis: Conception, review, and critique of the final manuscript.

Cleanthe Spanaki, MD, PhD*
Spiros Zafeiris, MD
Andreas Plaitakis, MD, PhD
Department of Neurology, University of Crete, Medical School, Heraklion, Crete, Greece
**E-mail: kliospanaki@yahoo.com*

References

1. van de Warrenburg BP, Bhatia KP, Quinn NP. Pisa syndrome after unilateral pallidotomy in Parkinson's disease: an unrecognised, delayed adverse event? J Neurol Neurosurg Psychiatry 2007;78: 329–30; Erattum in J Neurol Neurosurg Psychiatry 2008;79: 337.
2. Tolosa E, Compta Y. Dystonia in Parkinson's disease. J Neurol 2006;253 (Suppl 7):VII7–VII13.
3. Bhatia KP, Marsden CD. The behavioral and motor consequences of focal lesions of the basal ganglia in man. Brain 1994;117:859–876.
4. Heikkila RE, Shapiro BS, Duvoisin RC. The relationship between the loss of dopamine nerve terminals, striatal 3H-spiroperidol binding and rotational behavior in unilaterally-lesioned rats. Brain Res 1981;211:285–292.
5. Picconi B, Centonze D, Hakansson K, et al. Loss of bidirectional synaptic plasticity in L-dopa induced dyskinesias. Nat Neurosci 2003;6:501–506.
6. Fine J, Duff J, Chen R, Chir B, Hutchison W, Losano AM, Lang AE. Long-term follow-up of unilateral pallidotomy in advanced Parkinson's disease. N Engl J Med 2000;342:1708–1714.
7. Strutt AM, Lai EC, Jankovic J, et al. Five-years follow-up of unilateral posteroventral pallidotomy in Parkinson's disease. Surg Neurol 2009;71:551–558.

GPi-pallidal Stimulation to Treat Generalized Dystonia in Cockayne Syndrome

Video 

Cockayne syndrome (CS) is a rare autosomal recessive, progeroid disorder characterized by progressive multisystem degeneration.[1] While neurological impairments usually begin

Additional Supporting Information may be found in the online version of this article.

Potential conflict of interest: Nothing to report.

Published online 3 February 2010 in Wiley InterScience (www.interscience.wiley.com). DOI: 10.1002/mds.22992

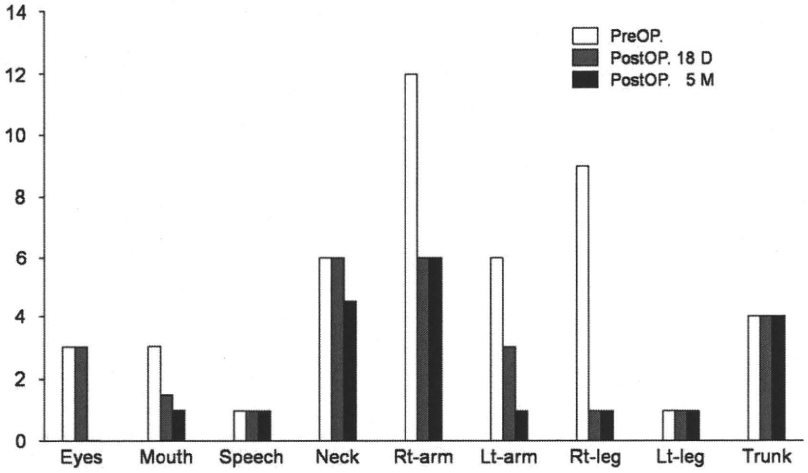

FIG. 1. Changes in the Burke-Fahn-Marsden Dystonia Rating Scale (BFM-DRS) subscores before and after surgery. During the 5 month of follow-up period, dystonic symptoms in the craniofacial region, neck, and extremities improve progressively. His total BFM-DRS score, 45 before treatment (maximum = 120) decreased to 26.5 (41.1% improvement) at 18 days and to 19.5 (56.7% improvement) at 5 months after the operation.

in early infancy,[1] CS spans a wide range of phenotypical expressions and a variable clinical course.[1,2] We describe our experience with the use of deep brain stimulation (DBS) for the bilateral globus pallidus internus (GPi) in a CS patient associated with generalized dystonia.

The patient, a 52-year-old man with growth failure manifesting cognitive disturbance (IQ = 44), microcephaly (head circumference = 48 cm), and low body height (155 cm) and weight (44 kg) also presented with retinal degeneration, cataract, and sensorineuroal hearing impairment, bilaterally. He had been born without perinatal complications as the 8th of 9 healthy siblings; however, abnormal growth and cognitive development became apparent before he entered elementary school. Around the age of 30 years, he began to manifest involuntary movements of his right arm; at the age of 33, he was placed in a nursing home. At the age of 42, he developed cervical dystonia (CD). Despite variable medical therapies, such as Clonazepam, Haloperidol, or Trihexyphenidyl combined with botulinum toxin injections, dystonia spread to his trunk and lower extremities, making walking difficult. Progressive CD severely interfered with his eating and he consequently suffered aspiration pneumonia in April 2008. On admission to our hospital, the patient received 2 mg/day of Clonazepam. He exhibited blephalospasm, oromandibular grimacing, CD with muscular pain, truncal bending and torsion, and dystonic tremor of the extremities. He was unable to hold out his hands horizontally. He could not grasp his right hand usefully, and his dystonic tremor and posture also severely interfered with eating with his left hand (Video Segment 1).

His preoperative Burke-Fahn-Marsden (BFM)-Dystonia Rating Scale (DRS) was 45/120 (Fig. 1). Neuroradiological studies showed extensive atrophy of the cortical and subcortical structures and the cerebellum without marked calcified lesions. We proceeded surgery after receiving prior informed consent from the patient and his family indicating uncertain outcome.

In June 2008, under general anesthesia, he underwent stereotactic implantation of DBS electrodes (model 3387; Medtronic) into the bilateral GPi. On the microelectrode recordings, the background activity was significantly reduced when the probe was passing through the point 2 mm anterior, 21 mm lateral, and 3 mm ventral to the midpoint of the anterior–posterior commissure line. Then, the contact 0 of the DBS electrode was placed at this target site.

His postoperative course was uneventful. Using the contacts 0 and 1, chronic unipolar stimulation (130 Hz frequency, 450 μsec pulse width) was started with pulse generators (Soletra, Medtronic) implanted in the subclavian portion. In the course of 1 month, the amplitude was gradually increased to 2.8 V. Dose of clonazepam was reduced to 1 mg/day postoperatively. During a 5-month follow-up period, his dystonic symptoms progressively improved (Fig. 1). His dystonic tremor responded promptly GPi stimulation (Video Segment 2) and his muscular neck and shoulder pain disappeared within several days. By 1 week after surgery, he could eat by himself using his left- and occasionally his right hand (Video Segment 2). The abnormal posture of his trunk did not change (Video Segments 1–3). His BFM-DRS decreased to 26.5/120 (41.1% improvement) at 18 days and to 19.5/120 (56.7% improvement) at 5 months.

The incidence of movement disorders associated with CS is not high; however, in their presence, they tend to be refractory to medical therapy.[1,3] Progressive pathologic changes in the basal ganglia-thalamocortical motor loop[4] may underlie the manifestation of abnormal movements in CS.[5]

In contrast to primary generalized dystonia, patients with secondary dystonia experienced less and more variable benefits from GPi-DBS.[6] However, it exerted considerable effects on generalized dystonia secondary to rare neurodegenerative syndromes such as pantothenate kinase-associated neurodegeneration.[7] These findings as well as ours strongly suggest

that even patients with decade-long dystonia due to progressive pathological and/or anatomical changes may derive benefits from this treatment.

As previously suggested, that is, phasic forms of dystonia may have a better improvement with DBS than tonic and fixed forms, dystonic tremor (and cervical muscular pain) responded promptly to GPi stimulation in our patient. His long-lasting spinal deformity might affected his mild but sustained abnormal posturing of the trunk.

Despite the secondary nature of dystonia, GPi-DBS exerted beneficial effects on daily living activities in our patient. Although additional case histories must be accumulated and long-term follow-up studies are needed to clarify optimal indications, our findings suggest DBS as a potential therapeutic option to treat movement disorders in CS.[3]

LEGENDS TO THE VIDEO

Segment 1. Preoperatively, the patient manifests continuous right-side dominant dystonic tremor of the extremities. He cannot hold his hands out horizontally and he is unable to grasp with his right hand. Note that his cervical and craniofacial dystonia is aggravated by actions tasked to the right hand (distant part of body). Tonic dystonia in his trunk and lower extremities interfere with his walk. There is severe interference in eating.

Segment 2. Eighteen days postoperatively, the dystonic tremor of the extremities disappeared. He can hold up both hands and use his right hand. Moderate cervical and craniofacial symptoms remain. His walk is steadier and he can eat by himself using his left- and occasionally his right hand.

Segment 3. After 5 months of continuous GPi stimulation, he can easily hold up both hands, although mild cervical dystonia is remained. He demonstrates that he can use chop sticks with his left hand and drink with either hand.

Acknowledgments: This work was supported by a Grant-in-Aid for Scientific Research from the Ministry of Education, Culture, Sports, Science, and Technology of Japan and a foundation subscribed by Hokuto Hospital, Obihiro, Hokkaido, Japan.

Kiyotoshi Hamasaki, MD
Kazumichi Yamada, MD, PhD*
Tadashi Hamasaki, MD, PhD
Jun-ichi Kuratsu, MD, PhD
Department of Neurosurgery
Graduate School of Medical Sciences
Kumamoto University
Kumamoto, Japan
**Email: yamadakazu@fc.kuh.kumamoto-u.ac.jp*

References

1. Nance MA, Berry SA. Cockayne syndrome: review of 140 cases. Am J Med Genet 1992;42:68–84.
2. Tan WH, Baris H, Robson CD, Kimonis VE. Cockayne syndrome: the developing phenotype. Am J Med Genet 2005;135:214–216.
3. Hebb OM, Guadet P, Mendes I. Deep brain stimulation to treat hyperkinetic symptoms of Cockayne syndrome. Mov Disord 2006;21:113–115.
4. Eltahawy HA, Saint-Cyr J, Giladi N, Lang AE, Lozano AM. Primary dystonia is more responsive than secondary dystonia to pallidal interventions: outcome after pallidotomy or pallidal deep brain stimulation. Neurosurgery 2004;54:613–619.
5. Rapin I, Weidenheim K, Lindenbaum Y, et al. Cockayne syndrome in adults: review with clinical and pathologic study of a new case. J Child Neurol 2006;21:991–1006.
6. Mink JW. The basal ganglia and involuntary movements: impaired inhibition of competing motor patterns. Arch Neurol 2003;60:1365–1368.
7. Castelnau P, Cif L, Valente EM, et al. Pallidal stimulation improves pantothenate-kinase-associated neurodegeneration. Ann Neurol 2005;57:738–740.

Acta Neurochir (2010) 152:997–1006
DOI 10.1007/s00701-010-0609-6

CLINICAL ARTICLE

A positive correlation between fractional white matter volume and the response of Parkinson disease patients to subthalamic stimulation

Tadashi Hamasaki · Kazumichi Yamada · Toshinori Hirai · Jun-ichi Kuratsu

Received: 29 August 2009 / Accepted: 1 February 2010 / Published online: 20 February 2010

Abstract
Background Since optimal patient selection is essential for the success of subthalamic nucleus (STN) stimulation, the identification of reliable outcome predictors is important. The purpose of this study was to identify new imaging characteristics sufficiently reliable to predict treatment results.
Method Using preoperative magnetic resonance imaging studies of 21 Parkinson disease (PD) patients treated by STN stimulation, we performed whole brain-based analysis of voxel-based morphometry (VBM) data. Intracranial structures segmented into the gray matter fraction (GMF), white matter fraction (WMF), and cerebrospinal fluid fraction (CSFF) were subjected to univariate and multivariate analysis of the correlation between fractional volumes and postoperative improvement rates using the Unified PD Rating Scale (UPDRS).
Findings At 3 months after surgery, the WMF was significantly correlated with improvement rated on the total UPDRS (p=0.006), UPDRS part II (activities of daily living; p=0.008), UPDRS part III (motor; p=0.005). In contrast, there was no significant correlation between the effect of STN stimulation and GMF or the effect of stimulation and CSFF. The WMF also showed a significant correlation with postoperative scores in the "on" drug and "on" stimulation state (total UPDRS, p=0.027; UPDRS part II, p=0.019; UPDRS part III, p=0.034).
Conclusions Our data indicate that patients with a larger white matter volume benefited from STN stimulation whereas the volume of other brain structures was not correlated with its effect. We posit that preserved connectivity between components of the basal ganglia-thalamocortical circuit may be required for the effectiveness of electrical stimulation. VBM may represent a powerful tool to predict the response of patients with advanced PD to STN stimulation.

Keywords Parkinson disease · Subthalamic stimulation · Voxel-based morphometry · White matter

Abbreviations

AC–PC	Anterior commissure–posterior commissure
ADL	Activities of daily living
BrF	Brain fraction
CNS	Central nervous system
CSFF	Cerebrospinal fluid fraction
DBS	Deep brain stimulation
GMF	Gray matter fraction
LEDD	Levodopa equivalent drug dose
MPRAGE	Three-dimensional magnetization-prepared rapid gradient-echo
MRI	Magnetic resonance imaging
PD	Parkinson disease
PDRP	Parkinson disease-related pattern
PET	Positron emission tomography
SMA	Supplementary motor area
STN	Subthalamic nucleus
UPDRS	Unified Parkinson's Disease Rating Scale
VBM	Voxel-based morphometry
WMF	White matter fraction

T. Hamasaki (✉) · K. Yamada · J.-i. Kuratsu
Department of Neurosurgery, Kumamoto University Medical School,
1-1-1 Honjo,
Kumamoto 860-8556, Japan
e-mail: thamasaki-nsu@umin.ac.jp

T. Hirai
Department of Diagnostic Imaging, Kumamoto University Medical School,
1-1-1 Honjo,
Kumamoto 860-8556, Japan